Reductions of NO_2 detected from space during the 2008 Beijing Olympic Games

B. Mijling,[1] R. J. van der A,[1] K. F. Boersma,[1] M. Van Roozendael,[2] I. De Smedt,[2] and H. M. Kelder[3]

Received 29 April 2009; accepted 27 May 2009; published 1 July 2009.

[1] During the 2008 Olympic and Paralympic Games in Beijing (from 8 August to 17 September), local authorities enforced strong measures to reduce air pollution during the events. To evaluate the direct effect of these measures, we use the tropospheric NO_2 column observations from the satellite instruments GOME-2 and OMI. We interpret these data against simulations from the regional chemistry transport model CHIMERE, based on a 2006 emission inventory, and find a reduction of NO_2 concentrations of approximately 60% above Beijing during the Olympic period. The air quality measures were especially effective in the Beijing area, but also noticeable in surrounding cities of Tianjin (30% reduction) and Shijiazhuang (20% reduction).
Citation: Mijling, B., R. J. van der A, K. F. Boersma, M. Van Roozendael, I. De Smedt, and H. M. Kelder (2009), Reductions of NO_2 detected from space during the 2008 Beijing Olympic Games, *Geophys. Res. Lett.*, *36*, L13801, doi:10.1029/2009GL038943.

1. Introduction

[2] Heavy air pollution in Beijing, mainly originating from dense traffic, construction activities, industry, and coal-fired power plants, is a major concern for local authorities. Important measures have been taken to prevent high levels of air pollution during the Beijing Olympic Games (8–24 August 2008) and the Paralympics (6–17 September 2008). In order to reduce anthropogenic emissions, the Beijing Municipal Environmental Protection Bureau (BJEPB) and Chinese newspapers report that traffic within the ring roads was restricted to cars with even number plates on even days and with odd numbers on odd days (from 20 July). 300.000 high-emission vehicles were banned from the city's roads (1 July) and the use of governmental and commercial vehicles was restricted (by 50% from 23 June; by 70% after 1 July). Access to specific roads (the ''Olympic Lanes'') was prohibited for other than Olympic related traffic. Public transport capacity was increased with the introduction of new metro and bus lines. Polluting industry was shut down temporarily (20 July) or rebuilt outside Beijing. Energy production in major coal-fired power plants was reduced by 30% and all construction activities were put on hold (20 July). Surrounding areas can contribute significantly to Beijing's air pollution [*Streets et al.*, 2007], hence similar (but less stringent) measures have been taken in the adjacent Hebei province and in Tianjin (110 km southeast of Beijing; ~11 million inhabitants). Most restrictions were lifted on 21 September.

[3] According to the BJEPB, the measures proved successful in reducing air pollution during the Olympic Games and the Paralympics (see Table 1): all days complied with the Grade II limit (a 24h averaged concentration of PM_{10} below 150 $\mu g/m^3$), and even 35% of the days complied with the Grade I limit (PM_{10} under 50 $\mu g/m^3$), as compared to the pre-Olympic period when only 3% of the days complied with the Grade I limit and 39% exceeded the Grade II limit.

[4] Precipitation data taken from the Unified Precipitation Project of the NOAA Climate Prediction Center [see *Chen et al.*, 2008] show that from 8 August to 17 September in Beijing 225 mm rain accumulated in 15 rainy days, substantially more than 73 and 91 mm in 6 and 7 rainy days for the same period in 2006 and 2007 respectively. Aviation weather reports from Beijing International Airport show a different prevailing wind direction (north instead of south to east), bringing in more clean air from the mountains.

[5] We will show here that significantly reduced air pollution in Beijing (in the form of NO_2 concentrations) is observed from space by the Global Ozone Monitoring Experiment 2 (GOME-2) and the Ozone Monitoring Instrument (OMI) during the Olympic period. To compensate for the atypical meteorological conditions, we use the satellite observations in combination with simulations of a regional transport model to obtain quantitative estimates of the reduction of NO_2 concentrations.

2. Satellite Observations and Simulations

[6] We use data of two satellite instruments: OMI, taking advantage of its high spatial resolution and daily global coverage, and GOME-2, taking advantage of a stronger anthropogenic NO_2 signal due to its earlier overpass in the day [*Boersma et al.*, 2008a]. Both instruments are nadir viewing spectrometers which measure the solar radiation backscattered by the Earth's atmosphere.

[7] GOME-2 is carried on the MetOp-A satellite which was launched in October 2006. It uses four channels to cover a spectral range from 240 to 790 nm. Slant columns of NO_2 are retrieved in the 425–450 nm spectral window. The instrument scans with a mirror mechanism 1920 km across track, therefore having near-global daily coverage. In forward scan its footprint is 80 × 40 km^2; overpass time is around 9:30 local time. OMI (on board the Aura satellite, launched on July 2004) measures in the spectral range from 270 to 500 nm with a spectral resolution of about 0.5 nm. Slant columns of NO_2 are retrieved in the 405–465 nm

[1]Royal Netherlands Meteorological Institute, De Bilt, Netherlands.
[2]Belgian Institute for Space Aeronomy, Brussels, Belgium.
[3]Department of Applied Physics, Eindhoven University of Technology, Eindhoven, Netherlands.

0094-8276/09/2009GL038943$05.00

Table 1. Overview of the Days Complying Air Quality Standards for PM_{10} for Different Periods From May to November 2008, According to BJEPB[a]

Period	Description	Days	Grade I 0–50 $\mu g/m^3$	Grade II 51–150 $\mu g/m^3$	Grade IIIa 151–250 $\mu g/m^3$	Grade IIIb–V >250 $\mu g/m^3$
2 May–30 June	pre-Olympic	60	2[b]	34[b]	15[b]	8[b]
1 July–7 Aug	transition	38	6[c]	21[c]	6[c]	0[c]
8 Aug–17 Sep	Olympic	41	14	26	1[d]	0
18 Sep–30 Nov	post-Olympic	74	18	43	11	2

[a]For all these days PM_{10} is the main pollutant. The standards are applied to the 24h mean of the surface concentration measured by 8 stations of the monitoring network. Data taken from www.bjepb.org.cn.
[b]Data missing for 24 May.
[c]Data missing for 3, 13–14, 16–17 July.
[d]At 29 August.

spectral window. The 114° viewing angle of the telescope corresponds to a 2600 km wide swath on the surface, enabling a daily global coverage of its measurements. Its spatial resolution is 24×13 km^2 in nadir, and increases to 68×14 km^2 at the swath edges (discarding the outer 5 pixels). Overpass time is around 13:30 local time.

[8] For both instruments the tropospheric NO_2 columns are retrieved with the approach described by *Boersma et al.* [2004]. Slant columns are assimilated in the TM4 chemistry transport model [*Dentener et al.*, 2003], which provides both the stratospheric NO_2 background field and the *a priori* profile needed for the calculation of the tropospheric air mass factor (AMF). The AMF further depends on the viewing angles, surface albedo, and cloud parameters (taken from FRESCO for GOME-2 and O_2-O_2 for OMI). The uncertainty in NO_2 columns for individual retrievals from both instruments is estimated at $0.5–1.5 \times 10^{15}$ molec/cm^2 from the spectral fitting and an additional relative error of 10%–40% from errors in the calculation of the AMF [*Boersma et al.*, 2004]. The OMI dataset was successfully validated by *Boersma et al.* [2008b]; more on GOME-2 validation can be found in the auxiliary material.[1]

[9] The regional chemistry transport model CHIMERE [*Schmidt et al.*, 2001; *Bessagnet et al.*, 2004] has been implemented over East Asia (18°N to 50°N and 102°E to 132°E), containing all important populated and industrialized areas of China. The horizontal resolution used for this domain is $0.25° \times 0.25°$, which for Beijing corresponds to 21×28 km^2 in longitude and latitude. CHIMERE simulates the atmosphere in 8 layers up to 500 hPa. The meteorological data is taken from the deterministic forecast of the European Centre for Medium-Range Weather Forecasts (ECMWF), which is given on 91 atmospheric layers for a horizontal resolution of approximately 25×25 km^2. The gas-phase chemistry is described by the reduced MELCHIOR scheme [*Derognat*, 2002]; aerosol processes are included according to *Bessagnet et al.* [2004]. The boundary conditions for the model domain are taken from monthly climatologies.

[10] In Europe, CHIMERE has been extensively intercompared to other urban air quality models [e.g., *Vautard et al.*, 2006] and evaluated against ground-based measurements and satellite data [e.g., *Blond et al.*, 2007]. For the Beijing area, validation results are provided in the auxiliary material, together with more information on the model implementation. The main source of model error originates from the emission estimates, which for China are rapidly outdated by strong trends in emissions due to increasing economic activity [*Van der A et al.*, 2008]. For our model implementation we selected the recent INTEX-B emission inventory by *Zhang et al.* [2009]. It covers Asia on a $0.5° \times 0.5°$ resolution, containing the yearly totals of SO_2, NO_x, CO, VOC, PM_{10}, $PM_{2.5}$, BC, and OC by 4 sectors (power, industry, residential, and transportation) for the year 2006. This inventory has been successfully validated during the INTEX-B campaign [*Zhang et al.*, 2008].

3. Method and Results

[11] We compare satellite observations to CHIMERE simulations using the INTEX-B emission inventory (which does not account for reductions associated with the Olympic Games or emission trends between 2006 and 2008). We conduct the simulation from 2 May to 30 November 2008. To account for the CHIMERE model ceiling, we extend the CHIMERE vertical NO_2 profiles with simulated profiles from the global CTM TM4 between 500 hPa and the tropopause. The error introduced by this extension is insignificant because the tropospheric NO_2 column is dominated by the contribution from the highly polluted Beijing boundary layer. We ensure consistency between the CHIMERE simulations and the satellite observations by interpolating the simulated concentration fields to the retrieval time and averaging over the spatial extent of the retrieval footprint. The observed and simulated column concentrations are gridded on a high resolution grid of $0.125° \times 0.125°$.

[12] The dependence of the satellite retrieval x_{sat} on *a priori* information can be removed by applying the averaging kernel $\mathbf{A}$ to the model profile $\mathbf{x}_{mod}$. Observation and simulation can now be compared by assuming $x_{sat} = (1-r_p)\ \alpha_0\ \mathbf{A}\cdot\mathbf{x}_{mod}$, in which α_0 corrects for the inconsistencies in the model and in the modeled emissions (the inventory being outdated, or errors made in the estimates of monthly, weekly and diurnal cycles), and r_p represents the concentration reduction due to the air quality measures in a period p with respect to a reference period. The mean ratio α_p between the collocated observations and simulations in a period p can be estimated by applying a weighted least squares method, from which the concentration reduction can be calculated with $r_p = 1 - \alpha_p/\alpha_0$.

[13] Due to prevailing cloudy conditions during the period of interest, also cloudy satellite retrievals are taken into account in order to collect sufficient samples for the Beijing area. For GOME-2 cloud fractions up to 20% are

[1]Auxiliary materials are available in the HTML. doi:10.1029/2009GL038943.

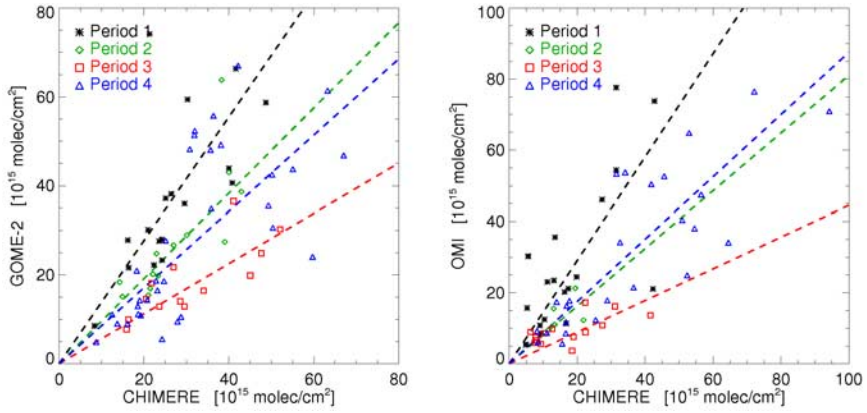

Figure 1. Relation between the corrected tropospheric NO_2 columns simulated by CHIMERE and observed (left) by GOME-2 and (right) by OMI for a $0.125^\circ \times 0.125^\circ$ grid cell over Beijing. For each period the best relation between model and satellite concentration has been fitted (dashed lines).

allowed, for OMI cloud fractions up to 40%. By discarding retrievals with clouds below 800 hPa, we avoid sensitivity problems of the retrieval when the cloud height intersects the NO_2 bulk.

[14] We distinguish 4 periods: a pre-Olympic period (2 May to 30 June 2008) that serves as a reference, a transition period (1 July to 7 August 2008) characterized by the enforcement of emission reductions, the Olympic period (8 August to 17 September 2008), and a post-Olympic period (18 September to 30 November 2008) when emission restrictions were supposedly lifted.

[15] The results for the grid cell containing the city center of Beijing are shown in Figure 1 and summarized in Table 2. In all periods the simulated and observed tropospheric NO_2 columns are well correlated: weighted correlation coefficients range from 0.55–0.82. This indicates that CHIMERE simulations capture the day-to-day variations in NO_2 driven by changes in meteorology and chemistry during these periods.

[16] The pre-Olympic period (before any air quality measures were enforced) spans 60 days in order to collect enough satellite data to act as a solid reference. Figure 1 shows that the satellite observations in this period are generally higher than the CHIMERE simulations, reflecting model biases and the NO_2 concentration trend between 2006 and 2008 [*van der A et al.*, 2008]. The concentration scaling factor α_0 is assumed to remain constant for all considered periods, because seasonal trends due to a changing chemical lifetime of NO_2 are taken into account by the model.

[17] In the transition period, GOME-2 and OMI show a reduction of column concentration of respectively 31% and 44% with respect to the previous period, indicating that the air quality measures are taking effect.

[18] In the Olympic period, the column concentration reduction is at its maximum, as expected. GOME-2 and OMI columns show a reduction of 59%–69% with respect to pre-Olympic values. Figure 2 shows the geographic extent of the concentration reductions as observed by GOME-2. In the pre-Olympic period both satellite and model show high concentrations in the populated and industrialized areas. During the Olympic period, the satellite observes decreased NO_2 concentrations for Beijing, whereas the other cities continue to show high concentrations. Highest concentration reductions are found in and around Beijing and the industrial areas in the south and south–east (60%–70%). The surrounding cities of Tianjin and Shijiazhuang show smaller reductions of ~30% and ~20%, respectively.

[19] The post-Olympic period shows an increase in NO_2 concentrations with respect to the Olympic period: in Beijing the concentration reductions are 38% for GOME-2 and 40% for OMI. The NO_2 concentrations do not return to their high pre-Olympic values.

[20] In the above method, we use the ratio of observed and simulated NO_2 columns in the pre-Olympic period as a reference to determine the concentration reductions during subsequent periods. This method relies on the skill of CHIMERE in accurately simulating the seasonal cycle over the Beijing region. As an alternative, we evaluate average NO_2 columns observed from space for corresponding periods in different years, see Figure 3. During the Olympic period, we find that GOME-2 observes over Beijing 46% less NO_2 in 2008 than in 2007. In the same period, OMI

Table 2. Overview of the Results of the Comparison Between CHIMERE and GOME-2 and OMI for Each Period for Beijing

	GOME-2			OMI		
Period	Days With Data	Weighted Correlation	Scaled Concentration Reduction r	Days With Data	Weighted Correlation	Scaled Concentration Reduction r
pre-Olympic	17	0.67	0	19	0.70	0
transition	13	0.76	31%	6	0.55	44%
Olympic	13	0.82	59%	14	0.72	69%
post-Olympic	34	0.60	38%	26	0.76	40%

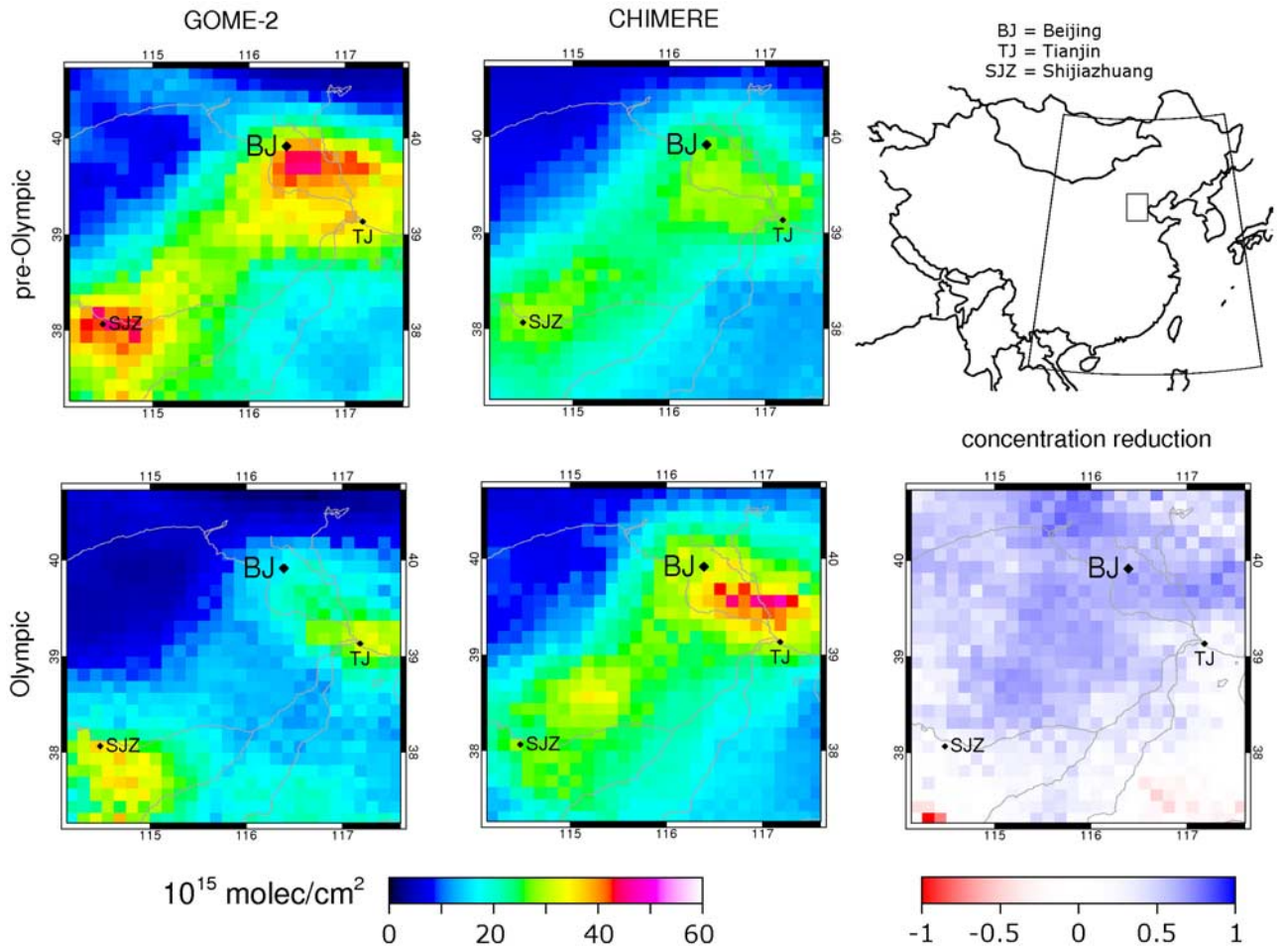

Figure 2. Tropospheric NO_2 columns during the pre-Olympic and Olympic periods, and the associated NO_2 reduction over the wider Beijing area (small box on map; large box indicates the CHIMERE domain). (left) GOME-2 tropospheric NO_2 column concentrations; (middle) corresponding CHIMERE simulations. (right) Associated concentration reduction: the air quality measures were especially effective in the area around Beijing (BJ); the cities of Tianjin (TJ) and Shijiazhuang (SJZ) showed smaller reductions in air pollution.

observes 59% less NO_2 in 2008 against the 2005–2007 average. For the post-Olympic period GOME-2 observes a reduction of 38% (consistent with the results of our model approach); OMI observes a 4% decrease against the 2005–2007 average.

4. Conclusion and Discussion

[21] Meteorological conditions during the 2008 Beijing Olympic Games were atypical. To study the effect of the air quality measures it is therefore essential to compare the air quality measurements with the simulations of a chemistry transport model. In this study, we use tropospheric NO_2 column retrievals of OMI and GOME-2, and implemented the CHIMERE model for East Asia based on the INTEX-B emission inventory.

[22] Comparison of the model with GOME-2 shows a reduction of 59% above Beijing with respect to pre-Olympic concentrations (with a high correlation coefficient of 0.82); OMI shows a reduction of 69% (with a correlation coefficient of 0.72). Earlier experiments by the Beijing authorities already showed the effectiveness of traffic reduction on the air quality. During the Sino-African summit in 2006, for example, traffic was reduced by an estimated 30% from 1 to 6 November, resulting in a 40% reduction in NO_x emissions [*Wang et al.*, 2007]. If a linear relationship is assumed between local NO_2 columns and local NO_x emissions (as shown by, e.g., *Martin et al.* [2006], and reaffirmed by experiments with our model) a 59%–69% concentration reduction in the Beijing area would correspond with similar reductions in NO_x emissions. This number seems plausible, although it is difficult to make an accurate estimate of the expected emission reduction directly from the long and diverse list of air quality measures. In any case, our results appear consistent with *Wang et al.* [2009] who report 36–55% reductions in NO_x emissions during the period of the Olympic Games compared with the same month one year earlier on in situ measurements and bottom-up estimates.

[23] The satellite measurements confirm that also outside Beijing (although to a lesser extent) measures have been effective: we find a concentration reduction of ~30% in Tianjin and ~20% in Shijiazhuang.

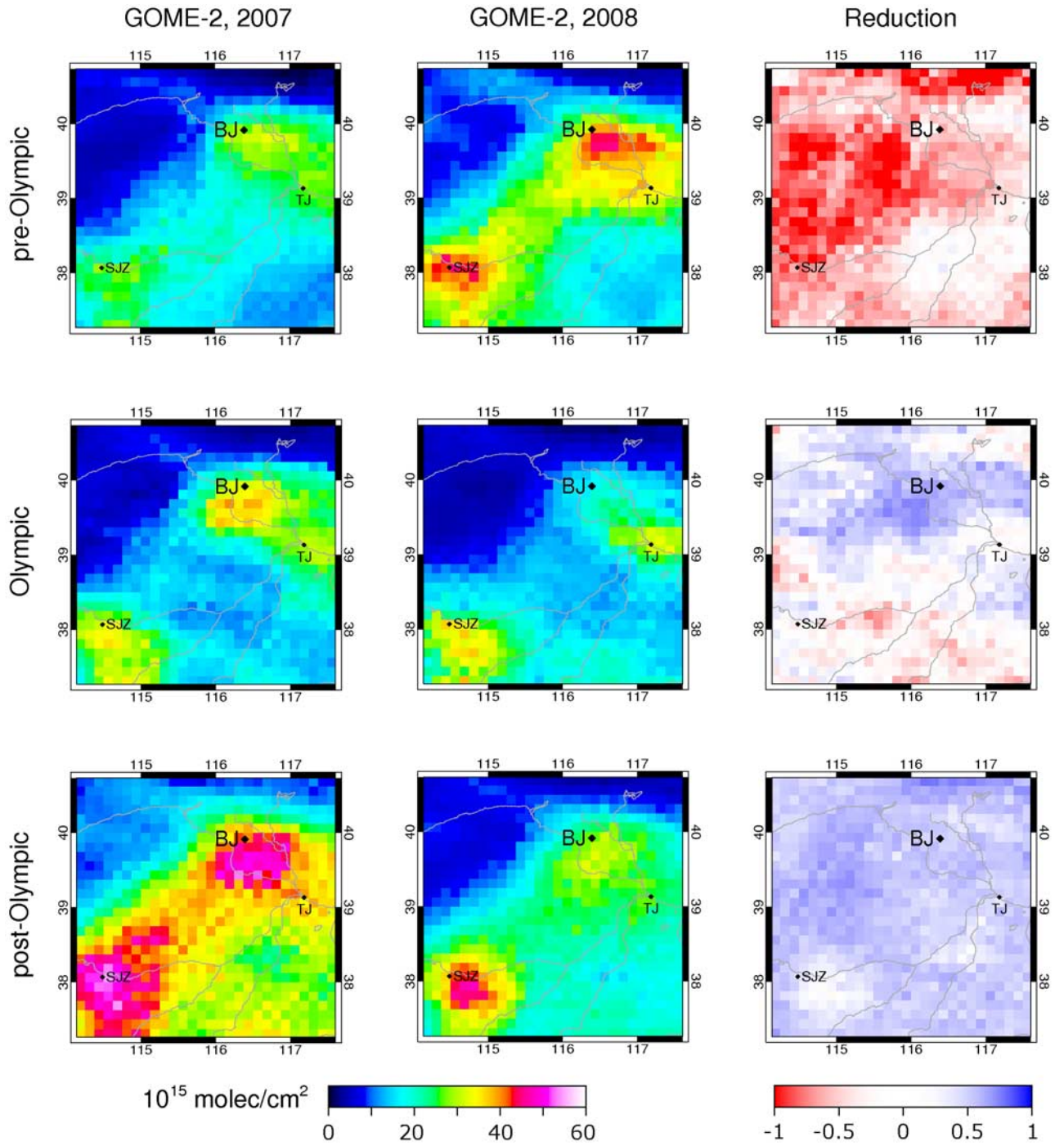

Figure 3. Tropospheric NO_2 columns observed by GOME-2 for (left) 2007 and (middle) 2008 for the pre-Olympic, Olympic and post-Olympic period. In the Olympic period, the strongest (right) concentration reductions are found around Beijing. Concentration reductions are still present in the post-Olympic period.

[24] Without the model, we find a NO_2 reduction of 46% over Beijing when comparing GOME-2 observations in the Olympic period in 2008 with the corresponding period in 2007; OMI observes 59% less NO_2 in 2008 against the 2005–2007 average. The annual variability in NO_2 for this period is very strong, as is the annual trend for Beijing, which makes it hard to estimate a reliable concentration reduction from satellite observations alone, but the results appear consistent with the model comparison.

[25] Our combined observation-model analysis indicates that in the post-Olympic period the NO_2 concentrations increase again, but are still reduced ~40% with respect to pre-Olympic values. This strong reduction is confirmed using only satellite measurements: GOME-2 observes 38% less NO_2 in 2008 than in 2007 for this period. This might indicate that after the Olympic Games the air quality in Beijing has improved systematically, or that economic activity is only slowly recovering.

[26] **Acknowledgments.** The authors would like to thank Q. Zhang and D. Streets for using their emission inventory. This research has been funded by the EU-FP6 project AMFIC.

References

Bessagnet, B., A. Hodzic, R. Vautard, M. Beekmann, S. Cheinet, C. Honoré, C. Liousse, and L. Rouïl (2004), Aerosol modeling with CHIMERE—Preliminary evaluation at the continental scale, *Atmos. Environ.*, *38*, 2803–2817.

Blond, N., K. F. Boersma, H. J. Eskes, R. J. van der A, M. Van Roozendael, I. De Smedt, G. Bergametti, and R. Vautard (2007), Intercomparison of SCIAMACHY nitrogen dioxide observations, in situ measurements and air quality modeling results over Western Europe, *J. Geophys. Res.*, *112*, D10311, doi:10.1029/2006JD007277.

Boersma, K. F., H. J. Eskes, and E. J. Brinksma (2004), Error analysis for tropospheric NO_2 retrieval from space, *J. Geophys. Res.*, *109*, D04311, doi:10.1029/2003JD003962.

Boersma, K. F., D. J. Jacob, H. J. Eskes, R. W. Pinder, and J. Wang (2008a), Intercomparison of SCIAMACHY and OMI tropospheric NO_2 columns: Observing the diurnal evolution of chemistry and emissions from space, *J. Geophys. Res.*, *113*, D16S26, doi:10.1029/2007JD008816.

Boersma, K. F., et al. (2008b), Validation of OMI tropospheric NO_2 observations during INTEX-B and application to constrain NO_x emissions over the eastern United States and Mexico, *Atmos. Environ.*, *42*, 4480–4497, doi:10.1016/j.atmosenv.2008.02.004.

Chen, M., W. Shi, P. Xie, V. B. S. Silva, V. E. Kousky, R. Wayne Higgins, and J. E. Janowiak (2008), Assessing objective techniques for gauge-based analyses of global daily precipitation, *J. Geophys. Res.*, *113*, D04110, doi:10.1029/2007JD009132.

Dentener, F., M. van Weele, M. Krol, S. Houweling, and P. van Velthoven (2003), Trends and inter-annual variability of methane emissions derived from 1979–1993 global CTM simulations, *Atmos. Chem. Phys.*, *3*, 73–88.

Derognat, C. (2002), Pollution photooxydante à l'échelle urbaine et interaction avec l'échelle régionale, Ph.D. thesis, Univ. of Paris VI, Paris.

Martin, R. V., C. E. Sioris, K. Chance, T. B. Ryerson, T. H. Bertram, P. J. Wooldridge, R. C. Cohen, J. A. Neuman, A. Swanson, and F. M. Flocke (2006), Evaluation of space-based constraints on global nitrogen oxide emissions with regional aircraft measurements over and downwind of eastern North America, *J. Geophys. Res.*, *111*, D15308, doi:10.1029/2005JD006680.

Schmidt, H., C. Derognat, R. Vautard, and M. Beekmann (2001), A comparison of simulated and observed ozone mixing ratios for the summer of 1998 in western Europe, *Atmos. Environ.*, *36*, 6277–6297.

Streets, D. G., et al. (2007), Air quality during the 2008 Beijing Olympic Games, *Atmos. Environ.*, *41*, 480–492, doi:10.1016/j.atmosenv.2006.08.046.

van der A, R. J., H. J. Eskes, K. F. Boersma, T. P. C. van Noije, M. Van Roozendael, I. De Smedt, D. H. M. U. Peters, and E. W. Meijer (2008), Trends, seasonal variability and dominant NO_x source derived from a ten year record of NO_2 measured from space, *J. Geophys. Res.*, *113*, D04302, doi:10.1029/2007JD009021.

Vautard, R., et al. (2006), Evaluation and intercomparison of ozone and PM_{10} simulations by several chemistry transport models over 4 European cities within the CityDelta project, *Atmos. Environ.*, *41*, 173–188.

Wang, Y., M. B. McElroy, K. F. Boersma, H. J. Eskes, and J. P. Veefkind (2007), Traffic restrictions associated with the Sino-African summit: Reductions of NO_x detected from space, *Geophys. Res. Lett.*, *34*, L08814, doi:10.1029/2007GL029326.

Wang, Y., J. Hao, M. B. McElroy, J. W. Munger, H. Ma, D. Chen, and C. P. Nielsen (2009), Ozone air quality during the 2008 Beijing Olympics—Effectiveness of emission restrictions, *Atmos. Chem. Phys. Discuss.*, *9*, 9927–9959.

Zhang, L., et al. (2008), Transpacific transport of ozone pollution and the effect of recent Asian emission increases on air quality in North America: An integrated analysis using satellite, aircraft, ozonesonde, and surface observations, *Atmos. Chem. Phys.*, *8*, 6117–6136.

Zhang, Q., et al. (2009), Asian emissions in 2006 for the NASA INTEX-B mission, *Atmos. Chem. Phys. Discuss.*, *9*, 4081–4139.

K. F. Boersma, B. Mijling, and R. J. van der A, Royal Netherlands Meteorological Institute, P.O. Box 201, NL-3730 AE De Bilt, Netherlands. (mijling@knmi.nl)

I. De Smedt and M. Van Roozendael, Belgian Institute for Space Aeronomy, Ringlaan-3-Avenue Circulaire, B-1180 Brussels, Belgium.

H. M. Kelder, Department of Applied Physics, Eindhoven University of Technology, Postbus 513, NL-5600 MB Eindhoven, Netherlands.